Capturing the Dynamics of Mechanical Knobs

Colin Swindells   Karon E. MacLean

Department of Computer Science, University of British Columbia, Canada
E-mail: swindell@cs.ubc.ca, maclean@cs.ubc.ca

Abstract

We present a novel experimental apparatus for the capture and replay of physical controls (mechanical knobs), as well as a set of acquired models and a design discussion related to the characterization approach taken here. Our work extends existing research by addressing problems surrounding identification of physical controls, including sensor gripping techniques for arbitrary target devices; and improved hardware and algorithm combinations for finer capture resolutions. Models were acquired from 5 real knobs, based on 2nd order model fits to torque and kinematic results of swept-sine excitations.

1   Introduction

Capturing and replaying the dynamics of physical controls enables designers to objectively compare and contrast haptic components such as detents, friction, and inertia. For example, we might like to combine the friction in one knob with the detents from another. By separately identifying attributes in each knob, a designer can then specify and prototype a third knob with the desired combination. This approach also allows us to isolate and study performance and preferences for subtle aspects of manual controls.

In this paper, we use our apparatus (shown in Figure 1) to build on previous work for capturing, modelling and replaying dynamics of physical controls, and extend acquisition methods to rotary devices. User studies for replay are published independently.

1.1   Background

We need to consider many constraints to characterize and render physical controls, including model structure, resolution, and physical form factor.

Model Structure: A 'black box' physical model with unknown internal structure, or a model with known, configurable variables? For many physical applications, much model structure is known a priori. Using known structures such as stiffness, friction, and inertia help a modelling algorithm fit measured data. A primary concern with this approach is the difficulty of choosing the most appropriate model; one might make a very good fit to an inappropriate model. This problem does not arise with the very generalizable approach of Miller & Colgate [7], who applied a
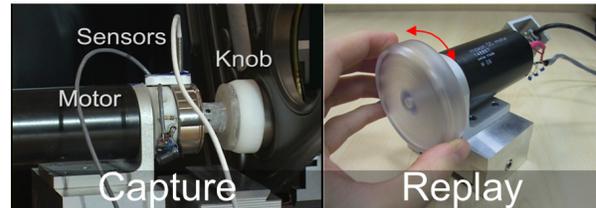

Figure 1: Capture & replay of knob dynamics

stimulus with varied frequency and power spectra, then built a 'black box' model in the frequency domain.

Nevertheless, simpler, structured models have the advantage of being highly consistent, which eases comparing different characterizations and helps designers think and work in terms of 'conceptual' model sub-elements with physical meaning, e.g. mechanical parameters of stiffness, friction, and inertia. Such an approach has been taken by others [1], [3], [5], [8], [9], [11]; an extreme case is the haptic profile of Weir et al. [12]. Instead of trying to fit all the subtle mechatronic dynamics to a mathematical model, Weir et al. made a tool to help designers build their own mental models and methods for comparing graphical plots derived from different mechatronic systems.

Model resolution: A many-parameters model addressing many subtle mechatronic details, or a few-parameters model addressing the most dominant mechatronic attributes? The most detailed model will not produce the best results because additional parameters will:

• Strain the fitting algorithm's ability to fit values to a certain level of consistency and quality. In non-linear curve fitting, for example, it is best to selectively apply non-linear techniques only to parts that require them.

• Jeopardize the rendering update rate, stability, and consistency of replayed mechatronic statics and dynamics. Replayed friction using a Karnopp model often feels better than that of more refined models (e.g. Stribeck [4]), and a small number of piecewise linear regions can be rendered more stably than many [5].

Physical form factor: What is the form being captured – switch or knob? One or many degrees of freedom (DOF)? Past efforts have focused on linear-acting devices because they are relatively easy to grip, whereas our group's work with knobs motivated us to

address the rotary problem. Can the capture be performed nondestructively in the target's environment – must a knob be removed from a car's dashboard and physically destroyed to capture its dynamics? How can the capturing and displaying devices be designed with a minimal transmission in order to maximize stiffness and reliability?

1.2 Approach

We demonstrate a system for capturing and replaying dynamics of mechanical knobs. Torque captures are presented for five mechanical knobs that were characterized using our custom rotary 'haptic camera' apparatus shown in Figure 2. These knobs were chosen to represent a variety of position, velocity, and acceleration dependent parameters with which to evaluate the effectiveness of our system.

The knob modeling process consisted of (a) exciting the knobs with precisely controlled swept-sine kinematic and torque trajectories while measuring torque and kinematics, respectively; then (b) estimating 2nd order model parameters using a non-linear least squares fit. To test the algorithm's accuracy, we characterized two simulated test knobs and compared the resulting parameter estimates to the known parameters of the simulated test knobs.
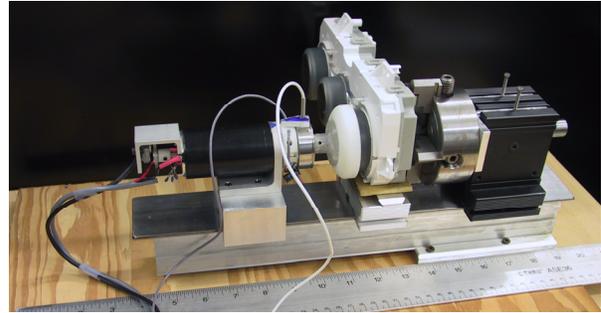
2 Rotary Haptic Camera Apparatus

Our haptic camera apparatus is an extension of similar mechanical characterization devices developed by MacLean [5], Colton & Hollerbach [1], and Richard [11]. The primary mechatronic extensions of this iteration are:

- *Resolution:* theoretical torque granularity as fine as 0.2 mNm is possible with the current setup.
- *Gravity compensation:* gravity often influences rotary accelerometer measurements.
- *Gripping:* we achieved a stiff physical coupling between the mechanical knob and haptic camera using custom designed plastic molds.
- *Rotary form factor:* previous work focused on characterizations along linear surfaces or switches.

2.1 Sensing

Table 1 lists spatial and torque sensing resolutions. Position was measured using a custom mounted encoder (MicroE M2000-M05-256-4-R1910-HA). Velocity was measured by differentiating the rotary position with respect to time and smoothing with a 10th order Butterworth IIR low-pass filter. We used a micromachined accelerometer (ADXL 202) in a custom ABS housing, and a strain-gauge-based rotary torque sensor (Honeywell-Sensotec QWFK-8M).

Figure 2: Rotary haptic camera physical setup

Sensor design efforts focussed on high resolutions, fast update rates, low mass, noise shielding and appropriate spatial placement. Low mass minimized introduction of extraneous dynamics. Locating apparatus mass off the torque sensor's active (i.e., gripping) end and tightly packing components improved sensitivity. Electrical and mechanical noise was minimized by using flexible medical-grade cables and stiff shaft couplings.

Table 1: Sensor resolutions

Position	Velocity	Acceleration	Torque
9.8×10^{-6} rad	2.0×10^{-4} rad/s	2.8 rad/s^2	1.8×10^{-4} Nm

2.2 Actuation

We used a ± 12 V DC motor (Maxon RE40) with a PWM amplifier (Copley 2122). We achieved smooth, responsive dynamic actuation by minimizing transmission components (no gears or cables). Capacitors on motor terminals reduced electronic noise. The actuator was chosen to provide enough torque to smoothly break the 'stuck' frictional state of a wide collection of physical controls (i.e., knobs). Maximum power available from a standard electrical socket provided an additional constraint.

2.3 Gravity Compensation

We compensated for gravity by measuring accelerometer voltages for 360º of each target knob, and fit a sine wave to these data. Gravity could then be compensated from any acceleration value by subtracting the calibration sine function's value at the current apparatus angle.

Although this approach was time consuming, other methods (double-differentiating position data or mounting the capturing apparatus to rotate orthogonal to gravity) were too noisy or too impractical for measuring knobs in their 'natural' environments, respectively.

2.4 Gripping

Excellent gripping was achieved with custom ABS (Acrylonitrile Butadiene Styrene) encasements for each

IEEE
COMPUTER
SOCIETY

target knob, using a 3D Solidworks model 'printed' by a Stratasys FDM Vantage i 3D printer. Each encasement was secured to its knob with industrial-grade double-sided tape. After capture, solvent released the encasements without damage.

Because the encasements attach to the sensing end of the torque sensor, they need low mass and high stiffness. While a chuck is more reusable, encasements were smaller, lighter, stiffer and less likely to damage delicate knob caps.

2.5 Physical Mounting

A small lathe bed provided a stiff, solid physical mounting base (Figure 2). Field measurements could be obtained by mounting the haptic camera assembly on a stiff tripod or custom clamp mechanism. The apparatus was designed for easy interchanging of test knobs. The actuator assembly slid from/to the target knob along the lathe bed. Micro-adjustment along both Cartesian axes perpendicular to the axis of rotation was achieved using a chuck.

2.6 Interfacing to a Computer

We found that capturing and replaying a physical control required relatively demanding computational resources: 5-10 kHz update rate, <20 µs variation between updates, and <20 ms lag.

A 3.0 GHz PC with 2 GB of RAM running a Timesys 4.0 Linux kernel was interfaced to the haptic camera via an I/O board, custom real-time middleware and a C++ controller [10]. During captures, we readily attained update rates of 5-10 kHz; however it was difficult to achieve < 10 µs latency for more than 99% of updates. Future versions should explore other realtime operating systems or embedded solutions.

3 Knob Model

Torque responses to a knob's acceleration, velocity, and position were fit to a non-linear least-squares model shown in Equation 1. We took a separable solution approach using Matlab's "lsqcurvefit" to fit P_{pos} and S_{pos}; and Matlab's "\" to fit M_{acc}, C_{vel-}, B_{vel-}, C_{vel+}, and A_{pos}. [6]. For function minimization we used the Levenberg-Marquardt method instead of the more traditional Gauss-Newton method (Gill et al. [2]).

Equation 1 illustrates the system model used for both system capture and replay of haptic knobs. Torque, position, velocity, and acceleration values were captured, and then fit to the parameters in Equation 1.

The top row of Equation 1 models inertia.

The middle row of Equation 1 models friction based on the Karnopp friction. It has a linearly increasing 'stuck' friction state based on position until a threshold torque is reached. Beyond this threshold torque, a

linearly increasing 'slip' state is rendered based on velocity [4]. The C_{vel-}, C_{vel+}, B_{vel-}, and B_{vel+} parameters define the dynamic and viscous friction regions of the Karnopp model. Additional Karnopp friction model parameters (Δv, D_{vel+}, & D_{vel-}) were obtained by fitting a rectangle based on point density on a torque vs. velocity plot (Figure 7). Before fitting these Karnopp parameters, we removed (subtracted) the acceleration- and position-dependent torques in Equation 1 to give a torque vs. velocity plot.

The bottom row of Equation 1 models detents using a sinusoid containing parameters for amplitude, period, and phase shift. Non-sinusoidal detents could be modelled using other functions such as a triangle waveform. Other useful position-based functions include one or more ramps or polynomials.

With this model, we emphasized usability, consistency, and simplicity. It is usable because its basic structure fits well with a designer's intuitive notions of detents, friction, and inertia. It is consistent because it models these elements in a form that ease comparisons with previous research. For example, a Stribeck model is theoretically more accurate than the Karnopp model, but the practical ability to both capture and replay the additional torque subtleties generally result in *worse* overall practical performance, here and in Richard et al. [11]. Colton & Hollerbach suggested a scheme to weight physical control data using non-linear curve fitting [1]. While a promising approach, it appears to be difficult to correctly allocate weightings to captured signal vs. noise.

$$\tau = \begin{aligned} & M_{acc}\ddot{\theta} + \\ & C_{vel-}\,\mathrm{sgn}\,\dot{\theta}_- + B_{vel-}\dot{\theta}_- + C_{vel+}\,\mathrm{sgn}\,\dot{\theta}_+ + B_{vel+}\dot{\theta}_+ + \\ & A_{pos}\sin\left(\theta/P_{pos} + S_{pos}\right) \end{aligned} \quad (1)$$

τ	Torque applied to the actuator *
$\theta, \dot{\theta}, \ddot{\theta}$	Position, velocity, and acceleration of the actuator (motor)
M_{acc}	Acceleration value (inertia)
C_{vel-}, C_{vel+}	Negative & positive dynamic friction
B_{vel-}, B_{vel+}	Negative & positive viscous friction
$A_{pos}, P_{pos}, S_{pos}$	Possible position parameters for amplitude, period, and phase shifts, to render detents.

Additional symbols (Karnopp model):

Δv	Zero velocity threshold
D_{vel-}, D_{vel+}	Negative and positive static friction torques

* Units are in mNm, radians, and seconds unless noted otherwise

IEEE COMPUTER SOCIETY

4 Capturing Knob Models

The capture began with a test of the algorithm on simulated data (§4.1). We then performed a variety of sensor tests and calibrations (§4.2), and finally captured the dynamics for a set of real knobs (§4.3).

4.1 Validation

We tested the effectiveness of the capture procedure by running our algorithm on simulated perfect and noisy data of typical mechanical knobs.

Generating test data: Our simulated model consisted of Equation 1 with parameters set to: $M_{acc} = 0.4$, $C_{vel-} = 1.5$, $C_{vel+} = 2.0$, $B_{vel-} = 1.0$, $B_{vel+} = 1.5$, $A_{pos} = 1.0$, $P_{pos} = 0.2$, $S_{pos} = 0.9$. Equation 2 describes the swept sine position waveform which, with its two derivatives, we used to 'excite' the simulated model and generate the respective simulated torque data sets using Equation 3.

$$\theta_n = c \sin\left[\frac{\pi}{b-a}\left(\frac{(b-a)\ t_n}{d} + a\right)^2 - a^2\right] \qquad (2)$$

$\theta_n, \dot{\theta}_n, \ddot{\theta}_n$ Simulated position, velocity & acceleration

t_n Time, where $t_n = \dfrac{n}{f_s}, n \in [1,\ 30,000]$

f_s Simulation sample rate, set to 5000 Hz.

(a,b,c,d) Constants set to (0, 1.5, 1.0, 3.0)

$$\tau_{noisy} = \tau + 4.0[rand(length(\tau)) - 0.5] \qquad (3)$$

τ_{noisy}, τ Noisy and perfect simulated torques

rand()   Random number between 0 and 1

length()   Number of torque values (used 30,000)

Fitting Test Data: We then fit the spatial and torque data using the separated non-linear least-squares procedure described in §3. For the torque signal with no added noise, parameter fits had negligible error. For the noisy data, parameter fits (still very good) are shown in Table 2. Overall, the success of these simulations gave us confidence in our process.

Table 2: Fit results for noisy simulated data

|	M_{acc}	A_{pos}	P_{pos}	S_{pos}	C_{vel-}	B_{vel-}	C_{vel+}	B_{vel+}
Target	0.4	1.0	0.2	0.9	1.5	1.0	2.0	1.5
Fit	0.398	1.008	0.199	0.884	1.512	0.999	1.992	1.500

Sensor testing: We calibrated our sensors by commanding the motor through desired trajectories for position, velocity, acceleration and torque, then comparing measured with desired values. Figure 5 shows the results for kinematic trajectories with no

gripper load (i.e., spun freely), according to Equation 2 with $(a,b,c,d) = (0.0, 1.5, 1.0, 3.0)$.

Figure 4 shows results of commanding a torque trajectory with gripper attached and locked, according to Equation 2 with $(a,b,c,d) = (0.0, 1.5, 0.02, 3.0)$.
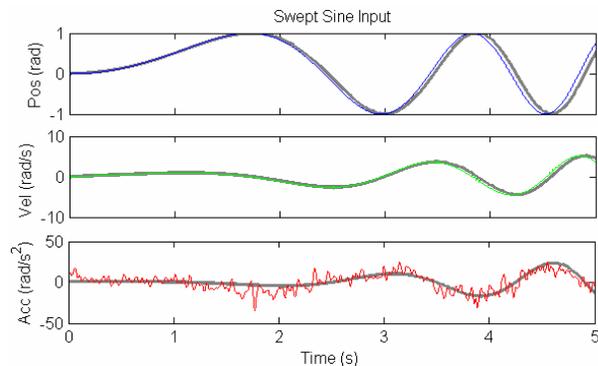
Figure 3: Original & measured spatial values
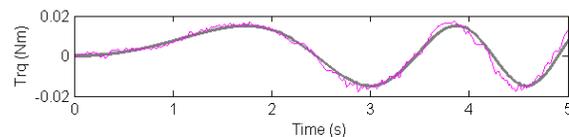
Figure 4: Original & measured torque values

Summary of test results: The measured results in Figures 3 & 4 match original values closely. The most notable discrepancy is a slight phase lag of < 1% (< 0.5 rad at 30 Hz) after 25,000 updates, for all four curves. Table 3 lists means and standard deviations of the differences between the original and measured values.

### Table 3: Differences between original and captured signals

	Position (rad)	Velocity (rad/s)	Acceleration (rad/s^2)	Torque (Nm)
Mean	0.0012	0.0016	0.664	0.0010
SD	0.0032	0.0244	0.4148	0.0018

## 4.2 Capture of 5 real knobs

Table 4 details the knobs, chosen to span a wide range of position, velocity, and acceleration effects. We

Table 4: Intuitive descriptions of test knobs

#	Description
1	Uniform position; moderate friction; low inertia
2	Uniform position; low friction; high inertia
3	Subtle detents; low friction; low inertia
4	Moderate detents; moderate friction; low inertia
5	Wide detents with backlash; moderate friction; low inertia (i.e., nonlinearities known to be inconsistent with Equation 1 – very difficult to fit)

IEEE COMPUTER SOCIETY
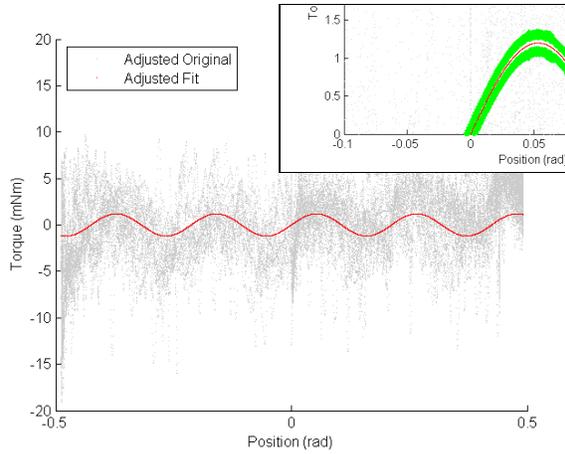
Figure 5: Example modeled torque vs. position overlaid on raw data (Knob 1) with 95% CI zoom
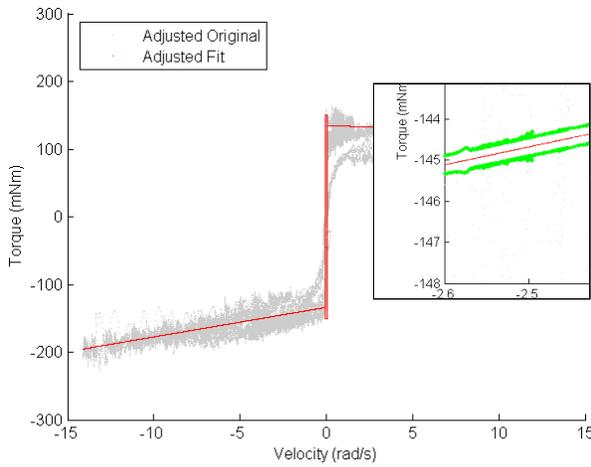
Figure 6: Example modeled torque vs. velocity overlaid on raw data (Knob 1) with 95% CI zoom

carried out two captures for each knob, each consisting of acquiring and analyzing one data set; the two were averaged into one model per knob.

Data preparation: Before fitting, the data was sorted by position [1], [11] and passed through a low pass filter to remove high-frequency noise. Third order Chebyshev type II IIR low pass filters with a stop band ripple of 20 dB were applied with the edge frequencies $(\theta, \dot{\theta}, \ddot{\theta}, \tau) = (1, 1, 0.5, 0.5)$ kHz. Phase shifts were avoided by using a two-stage, acausal filter (i.e., *filtfilt* in Matlab).

Fit results: Table 5 lists the mean of fit values taken from position, velocity, and acceleration excitations using two independent captures of each test knob. Table 6 lists mean of Karnopp friction model parameters manually read from torque vs. velocity views of the data such as that shown in Figure 9. Our main method of validating the capture of real knobs is

a 95% confidence interval to the fit data (i.e., *nlpredci* in Matlab). A small confidence interval size corresponds to a greater likelihood that the true model parameter is close to the fit value (more accurate).

Table 5: Mean of fit values from two independent captures for 5 knobs

Parameter	Knob 1	Knob 2	Knob 3	Knob 4	Knob 5
M_{acc}	0.091	0.28	0.035	0.049	0.0019
C_{vel-}	-46	-8.4	-2.3	-0.61	-19
B_{vel-}	2.7	-0.095	-0.15	0.55	4.7
C_{vel+}	46	8.4	2.3	0.61	19
B_{vel+}	-4.5	0.54	-0.24	0.28	4.1
A_{pos}	N/A	N/A	1.1	-11	-130
P_{pos}	N/A	N/A	0.034	0.076	0.10
S_{pos}	N/A	N/A	0.16	-0.20	-1.0
95% CI	0.30	0.19	0.091	0.073	4.2

Table 6: Means of Karnopp friction parameters read manually from torque/velocity plots

Parameter	Knob 1	Knob 2	Knob 3	Knob 4	Knob 5
D_{vel-}	-150	-17	-10	-20	-200
D_{vel+}	150	17	10	20	200
Δv	0.040	0.015	0.010	0.010	0.015

4.3 Knob Fit Analysis

Figures 5 & 6 represent typical torque vs. position and vs. velocity plots, respectively. The zoomed views of the 95% CI in these figures are typical of the good quality fits obtained for knobs 1–4 (i.e., 95% CI torque bounds are near the fit torque values). Segmentation of position, velocity, and acceleration components was successful, even for subtle properties such as the 0.5 mNm amplitude detents of Knob 3 (e.g., Figures 5 & 6 have the expected sinusoid & 'S' shapes, respectively). Finally, even though Knob 5's true structure significantly deviated from that defined by Equation 1 (e.g., strong non-sinusoidal detents and backlash can be felt when turning Knob 5), fits within a mean deviation of 4.2 mNm were still obtained (Table 5), implying that this algorithm was able to identify its defined structural elements even in the presence of certain types of unmodelled elements. Mean 95% CI magnitudes for Knob 5 were over 10x greater than magnitudes for Knobs 1-4 (Table 5), by contrast suggesting good quality fits for Knobs 1-4. Fit quality can also be compared to alternative independent tests. For example, P_{pos} can be estimated by turning the test knob and counting the detents over 360º (they agreed
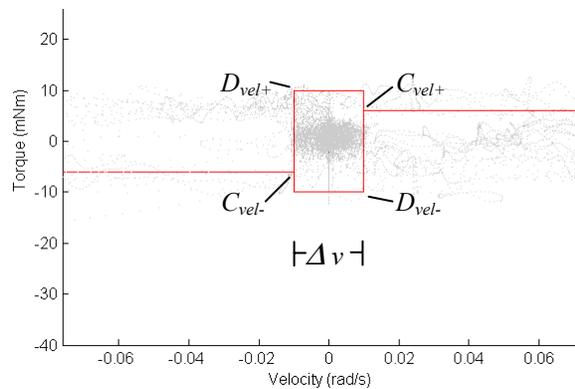
Figure 7: Static friction estimation for Knob 3

within 4.8%, 1.6%, & 9.9% for knobs 3, 4, & 5, respectively). Altogether, these results suggest a relative robustness to the capture and replay procedure. Complete data sets are in a technical report[1].

5   Conclusions and Future Work

Overall, the presented capture technique worked well, and models could be effectively rendered on a haptic knob. Major areas for future research are (i) development and use of better numerical analysis theory for non-linear curve fitting, and (ii) further refinement of apparatus spatial and temporal resolutions. Primary numerical analysis bottlenecks are sensitivity to algorithm parameters such as initial conditions, and difficulty in handling many unknown parameters – which would be needed to successfully parameterize more complex inertia, friction, and detent models. Nevertheless, the curve fitting techniques to isolate components that are intuitive to designers, such as inertia, friction, and detents, appear to work well enough for practical use in industry.

Although the spatial and temporal resolutions for our apparatus met or exceeded values of the best previous research, further enhancements would still be worthwhile. For example, acceleration values could possibly be improved using a sensor fusion approach combining an accelerometer with the 2nd derivative data from a very high resolution position sensor (> 1 million CPR). Although our encasements were of negligible mass, inertia for gripper encasements could be pre-calculated and subtracted from a fit model. Controlling fast, forceful swept input signals was sometimes difficult when attached to knobs (i.e., an unknown system). Although difficult to achieve, update rates of > 10 kHz with < 100 ns variation between updates, and lag times < 10 ms are technically

possible and would improve actuator control. Torque sensor dynamic range is also a concern. The best torque sensors currently provide ~1000 data points, so capturing a physical control with very stiff and very subtle torque attributes would either (i) damage a sensitive torque sensor, or (ii) require an overly coarse torque sensor incapable of measuring subtleties.

The described techniques would be generally applicable to capture and replay of physical controls such as knobs, sliders, and buttons. We are currently performing user tests to compare and validate human perception estimates of position, velocity, and acceleration parameters with their system identified equivalents for the same collection of 5 test knobs.

References

[1]   Colton, M.B., & Hollerbach, J.M. Identification of Nonlinear Passive Devices for Haptic Simulations. *Haptic Interfaces for Virtual Environment and Teleoperator Systems*, 2005.

[2]   Gill, P.R., Murray, W., and Wright, M.H.. *Practical Optimization*. Academic Press, 1981, 136 - 137.

[3]   Hasser, C.J., & Cutkosky, M.R. System identification of the human hand grasping a haptic knob. *IEEE Symposium on Haptic Interfaces for Virtual Environment and Teleoperator Systems (HAPTICS),* 2002.

[4]   Karnopp, D. Computer simulation of stick-slip friction in mechanical dynamic systems. *ASME Journal of Dynamic Systems, Measurement and Control, 10*, 1985.

[5]   MacLean, K.M. The 'Haptic Camera': A Technique for Characterizing and Playing Back Haptic Properties of Real Environments. *ASME Symposium on Haptic Interfaces for Virtual Environments and Teleoperator Systems (HAPTICS)*, 1996.

[6]   Mathworks, Inc. (2005, July 19). *Solution Number: 1-18E03*. Available at: http://www.mathworks.com/support/solutions/data/1-18E03.html?product=OP&solution=1-18E03.

[7]   Miller, B.E., & Colgate, J.E. Using a Wavelet Network to Characterize Real Environment for Haptic Display. *ASME Dynamic Systems and Control Division,* 1998.

[8]   Nagurka, M. & Marklin, R. Measurement of Impedance Characteristics of Computer Keyboard Keys, *IEEE Mediterranean Conference on Control and Automation (MEDS)*, 1999.

[9]   Novak, K.E., Miller, L.E., & Houk, J.C. Kinematic properties of rapid hand movements in a knob turning task. *Experimental Brain Research, 132*(4), 2000.

[10] Pava, G., MacLean, K. Real Time Platform Middleware for Transparent Prototyping of Haptic Applications. *IEEE Symposium on Haptic Interfaces for Virtual Environment and Teleoperator Systems (HAPTICS)*, 2004.

[11] Richard, C., Cutkosky, M.R., & MacLean, K.M. Friction Identification for Haptic Display. *ASME Sympmposium on Haptic Interfaces for Virtual Environment and Teleoperator Systems (HAPTICS)*, 1999.

[12] Weir, D.W., Peshkin, M., Colgate, J.E., Buttolo, P., Rankin, J., & Johnston, M. The Haptic Profile: Capturing the Feel of Switches. *IEEE Symposium on Haptic Interfaces for Virtual Environment and Teleoperator Systems (HAPTICS)*, 2004.

---

[1]   Tech   Report   TR-2006-14.   Available   at: http://www.cs.ubc.ca/tr